LBNL-45204
Preprint

ERNEST ORLANDO LAWRENCE
BERKELEY NATIONAL LABORATORY

Molecular Thermodynamics for Partitioning of Native and Denatured Proteins in Aqueous Two-Phase Systems

J. Jiang and J.M. Prausnitz

Chemical Sciences Division

February 2000

Submitted to
Journal of Physical Chemistry

REFERENCE COPY
Does Not
Circulate
Bldg. 50 Library - Ref.
Lawrence Berkeley National Laboratory

LBNL-45204
Copy 1

DISCLAIMER

This document was prepared as an account of work sponsored by the United States Government. While this document is believed to contain correct information, neither the United States Government nor any agency thereof, nor the Regents of the University of California, nor any of their employees, makes any warranty, express or implied, or assumes any legal responsibility for the accuracy, completeness, or usefulness of any information, apparatus, product, or process disclosed, or represents that its use would not infringe privately owned rights. Reference herein to any specific commercial product, process, or service by its trade name, trademark, manufacturer, or otherwise, does not necessarily constitute or imply its endorsement, recommendation, or favoring by the United States Government or any agency thereof, or the Regents of the University of California. The views and opinions of authors expressed herein do not necessarily state or reflect those of the United States Government or any agency thereof or the Regents of the University of California.

LBNL-45204

Molecular Thermodynamics for Partitioning of Native and Denatured Proteins in Aqueous Two-Phase Systems

J. Jiang and J.M. Prausnitz

Department of Chemical Engineering
University of California, Berkeley

and

Chemical Sciences Division
Ernest Orlando Lawrence Berkeley National Laboratory
University of California
Berkeley, California 94720

February 2000

This work was supported by the Director, Office of Science, Office of Basic Energy Sciences, Chemical Sciences Division, of the U.S. Department of Energy under Contract No. DE-AC03-76SF00098.

Molecular Thermodynamics for Partitioning of Native and Denatured Proteins in Aqueous Two-Phase Systems

Jianwen Jiang and John M. Prausnitz*

Chemical Engineering Department, University of California, Berkeley
and Chemical Sciences Division, Lawrence Berkeley National Laboratory, Berkeley, CA 94720

A molecular-thermodynamic analysis of protein partitioning in an aqueous two-phase system shows that the partition coefficient for a native (globular) protein is very much different from that for a denatured (linear) protein; while the former is weakly dependent on protein molecular weight, the latter depends strongly on molecular weight. The native protein and the denatured protein are represented, respectively, by a spherical macroion and by a linear flexible polyion. Based on McMillan-Mayer solution theory, the interactions between particles are represented by a continuum-averaged potential of mean-force containing hard-sphere repulsion, the effect of penetration or hydration forces, electrostatic interactions, osmotic attraction and specific interactions. Phase diagrams are calculated for polymer-polymer and for polymer-salt aqueous two-phase-forming systems in good agreement with experiment. Coupled with measured data for obtaining model parameters, partition coefficients are calculated for a native protein, lysozyme. Calculated partition coefficients for a denatured protein are compared with experimental partitioning data for short peptides. Calculated results are remarkably similar to those observed.

* To whom correspondence should be addressed.

1. Introduction

While aqueous two-phase systems were discovered 100 years ago,[1] their general application for purification of biomolecules was first described by Albertsson in the 1950s.[2,3] Albertsson showed that two-liquid aqueous phases can form in an aqueous solution that contains either two polymers or one polymer and one salt. When a protein is added, the protein partitions between the two phases with a partition coefficient that often deviates appreciably from unity.

Aqueous two-phase systems possess several advantages;[4] for example, because each phase contains predominantly water (75–90 wt%), the system has low interfacial tension thereby providing a mild environment for labile proteins. Thus, aqueous two-phase systems provide a powerful technique for separating complex mixtures of a wide range of biomolecules,[5-7] such as, proteins, amino acids, lipids, nucleic acids, viruses, plant and animal cells, etc.[8-11] Aqueous two-phase systems have been used for extractive fermentation or for enzyme reactions;[12] for characterizing hydrophobic[13,14] or binding interactions;[15,16] and for assays using Partition Affinity Ligand Assay (PALA).[17]

Polyethylene glycol (PEG) and dextran (DEX) are frequently used to form aqueous two-phase systems for biomolecule partitioning; PEG and salt are also used.[8] Recently, some new types of phase-forming systems have emerged, for example, copolymer with homopolymer;[18-21] copolymer with salt;[22] polymer with surfactant, or surfactant with surfactant.[23-25] Alternately, an aqueous two-phase system with only one surfactant[26-28] can be used to partition proteins with a number of desirable features when compared with traditional phase-forming systems.

The partitioning behavior of a biomolecule in an aqueous two-phase system is governed by several factors. For example, in a system containing two polymers, the effect of the molecular weight of phase-forming polymers is such that when the molecular weight of one polymer is decreased, the biomolecule tends to favor the phase rich in this polymer.[29,30] On the other hand, subtle changes in size, charge and surface chemistry of a biomolecule can also lead to noticeable changes in partitioning behavior.[31-35] Further, the structure or conformation of a biomolecule has much influence on its partitioning in aqueous two-phase systems. For example, native and denatured DNA,[36-38] and supercoiled and un-supercoiled DNA,[39,40] display very different partitioning behavior, as do linear and cyclic oligosaccharides.[41] Short peptides formed with various numbers of amino acids also show partitioning behavior quite different from that for native proteins.[42-47]

Industrial equipment design for separation and purification of biomolecules in aqueous two-phase systems is based on trial-and-error experiments. To aid design and to optimize aqueous two-phase systems for separation and purification of biomolecules, several theories have been proposed for predicting thermodynamic properties and phase behavior of phase-forming systems and partitioning behavior of biomolecules. Following a brief review (for detailed reviews, see Refs. 48-50), we present a new molecular-thermodynamic description of partitioning with emphasis on native and denatured proteins in aqueous two-phase systems.

Early attempts were reported by Brooks et al.[51] and by Tjerneld et al.[52] using Flory-Huggins (FH) lattice theory[53] to correlate qualitatively phase diagrams and protein partition-coefficient data in an aqueous mixture containing two polymer solutes. Diamond and Hsu[54] used a linearized form of FH theory to obtain a semiempirical expression for protein partitioning in polymer/polymer aqueous two-phase systems with or without salt buffer. Also, Hino and Prausnitz[55] applied FH theory to calculate phase separation in polymer/salt aqueous solutions.

Based on Scheutjens-Fleer lattice theory for polymer adsorption,[56] Baskir and coworkers[57] developed a modified lattice theory to predict protein partitioning without, however, accounting for salt effects. This description coupled with a Pitzer-Li long-range electrostatic term,[58] was extended by Li et al.[59] for partitioning of amino acids and proteins in polymer/salt system. In the same spirit, the polymer-scaling concept of de Gennes[60] was applied by Abbott et al.[61-63] to describe the interactions between protein with flexible, water-soluble nonionic phase-forming polymers toward describing protein partitioning.

The osmotic virial expansion, first proposed by Edmond and Ogston,[64] provided a simple theoretical framework[65] that is commonly used for aqueous two-phase systems. On this basis, King et al.[66] and Haynes et al.[67,68] predicted phase separation and protein partitioning in polymer/polymer systems in the presence or absence of salts. Similar studies were reported by Arai et al.[69] for amino acids partitioning in aqueous polymer/polymer systems, and by Zhu et al.[70] for phase separation in aqueous polymer/salt systems. Gaube et al. developed a thermodynamically-consistent osmotic virial expansion to predict phase diagrams of PEG/DEX[71-73] and PEG/sodium sulfate (Na_2SO_4).[74] These studies using the osmotic virial expansion were based on the McMillan-Mayer solution theory.[75] In contrast, based on the constant-pressure-solution theory of Hill,[76] Cabezas et al.[77-79] and Forciniti and Hall[80] developed an isothermal-isobaric virial expansion to study phase behavior of aqueous two-phase systems.

Kang and Sandler[81] used the UNIQUAC model[82] to predict binodals of polydisperse PEG/DEX aqueous two-phase systems. Combining Guggenheim's extension[83] of Debye-Hückel theory for long-range electrostatic interaction, Hartounian et al.[84] studied phase behavior and protein partitioning in the PEG/DEX system with a salt buffer. Similarly, the UNIFAC model[85] was used by Li et al.[86] to predict phase behavior of polymer/salt systems; a semiempirical group-contribution model was used to study amino acids and short-peptide partitioning in polymer/polymer and polymer/salt systems.[42-45]

Integral-equation theory has been applied by Haynes et al.[87,88] and by Kenkare and Hall[89] to study phase behavior and partitioning behavior of proteins in both aqueous polymer/polymer and aqueous polymer/salt two-phase systems.

These theoretical models were restricted to investigating partitioning behavior of native proteins, amino acids or short peptides in aqueous two-phase systems. To our best knowledge, however, no theoretical study has been reported for partitioning behavior of denatured proteins whose partitioning behavior is significantly different from that of native proteins.

In this work we present a molecular-thermodynamic model based on the McMillan-Mayer solution theory[75] where the dominant component in the aqueous two-phase system, water, is considered to be a continuous medium; interactions between solute molecules in this medium are represented by potential of mean-force. First, we consider phase separation in aqueous PEG 3000/DEX T500 with or without Na_2SO_4 buffer and second, we consider aqueous PEG 3000/Na_2SO_4 two-phase systems. We then consider the partitioning behavior of native and denatured proteins at conditions where the proteins are at infinite dilution.

2. Theoretical Framework

An aqueous two-phase system contains one or two polymers, electrolyte (salt), protein and water. Polymers and ions are represented, respectively, by attractive hard spheres and by charged hard spheres. A native protein is represented by a spherical macroion and a denatured protein by a linear, flexible, partially charged, polyion chain containing randomly distributed charged hard spheres and neutral hard spheres. The counterion of the protein is assumed to be identical to the corresponding ion of the salt. In the continuum, water, each particle k (for a polyion, k refers to its monomer before polyion-chain formation) has number density ρ_k and diameter σ_k. Particle k has charge $Z_k e$ (e is the charge of a proton). The entire system is subject to electroneutrality:

$$\sum_k \rho_k Z_k = 0. \tag{1}$$

Within the McMillan-Mayer framework, we must specify the continuum-averaged potential of mean force. For aqueous two-phase systems studied here, in addition to hard-sphere repulsion and electrostatics, several other essential interactions need to be considered. In the solution, the polymer is assumed to be in a random-coil configuration, allowing other particles partially to penetrate its average volume.[61] This polymer penetration effect can significantly influence the phase diagram for protein partitioning.[87,88] In some cases, however, there may be an impenetrable layer of water surrounding particles due to hydration.[90] In an aqueous polymer/salt solution with concentrated salt, ions occupy a significant fraction of the total volume; therefore, there may be an imbalance in the local osmotic pressure on the large particles (polymer or protein) exerted by the ions[91,92] leading to short-range osmotic attraction.[93,94] Finally, there may be some specific short-range interactions between particles, such as hydrogen bonding or association.[95]

The Helmholtz energy can be written as

$$A = A^{id} + A^{ex} \tag{2}$$

The contribution from ideal-gas mixing is

$$\frac{\beta A^{id}}{V} = \sum_k \rho_k \ln(\rho_k \Lambda_k^3) - \sum_k \rho_k \tag{3}$$

where $\beta = 1/k_B T$ (k_B is Boltzmann constant and T is temperature); ρ_k is the number density of molecules and Λ_k denotes de Broglie wavelength. All others contributions are excess Helmholtz energies obtained from perturbation theory:

$$A^{ex} = A^{hs} + A^{na} + A^{ele} + A^{oa} + A^{ve} + A^{ch}. \tag{4}$$

The BMCSL equation given by Boublik and Mansoori et al.[96] is used to calculated the hard-sphere contribution from polymer, or salt or protein:

$$\frac{\beta A^{hs}}{V} = (\zeta_2^3/\zeta_3^2 - \zeta_0)\ln\Delta + \frac{\pi\zeta_1\zeta_2/2 - \zeta_2^3/\zeta_3^2}{\Delta} + \frac{\zeta_2^3/\zeta_3^2}{\Delta^2} \tag{5}$$

where V is the total volume of the system; $\zeta_n = \sum_k \rho_k \sigma_k^n$; $\Delta = 1 - \pi\zeta_3/6$. Eq. 5 is based on the additive assumption $\sigma_{ij} = (\sigma_i + \sigma_j)/2$.

Due to polymer penetration or hydration, the collision distance d_{ij} between polymer i and particle j may be smaller or larger than the additive hard-sphere diameter σ_{ij}. Using a nonadditive parameter δ_{ij} defined by $d_{ij}=\sigma_{ij}(1-\delta_{ij})$, perturbation theory provides an estimate for A^{na}:[97]

$$\frac{\beta A^{na}}{V} = -2\pi \sum_i \sum_j \rho_i \rho_j \sigma_{ij}^3 \delta_{ij} g_{ij}^{hs}(\sigma_{ij}) \tag{6}$$

where $g_{ij}^{hs}(\sigma_{ij})$ is the contact value of the pair correlation function for an additive hard-sphere mixture,

$$g_{ij}^{hs}(\sigma_{ij}) = \frac{1}{\Delta} + \frac{\pi \sigma_i \sigma_j \zeta_2}{4\Delta^2 \sigma_{ij}} + \frac{\pi^2 \sigma_i^2 \sigma_j^2 \zeta_2^2}{72\Delta^3 \sigma_{ij}^2}. \tag{7}$$

The contribution from electrostatic interactions is obtained using the mean-spherical approximation (MSA):[98]

$$\frac{\beta A^{ele}}{V} = -\frac{\alpha_0^2}{4\pi}\left(\sum_k \frac{\rho_k Z_k^2 \Gamma}{1+\Gamma\sigma_k} + \frac{\pi P_n}{2\Delta}\sum_k \frac{\rho_k \sigma_k Z_k}{1+\Gamma\sigma_k}\right) + \frac{\Gamma^3}{3\pi} \tag{8}$$

where $\alpha_0^2 = \beta e^2/\varepsilon$ is the Bjerrum length characterizing the dielectric property of the continuum with dielectric permittivity $\varepsilon = \varepsilon_0 \varepsilon_r$ (ε_0 is the vacuum permittivity and ε_r is the dielectric constant). Γ is the scaling parameter obtained from

$$4\Gamma^2 = \alpha_0^2 \sum_k \rho_k \left(\frac{1}{1+\Gamma\sigma_k}\right)^2 \left(Z_k - \frac{\pi P_n \sigma_k^2}{2\Delta}\right)^2 \tag{9}$$

$$P_n = \sum_k \frac{\rho_k \sigma_k Z_k}{1+\Gamma\sigma_k} \Big/ \left(1 + \frac{\pi}{2\Delta}\sum_k \frac{\rho_k \sigma_k^3}{1+\Gamma\sigma_k}\right). \tag{10}$$

As shown in Appendix A, for osmotic attraction in an aqueous polymer/salt solution, where we use the random-phase approximation, the contribution to the Helmholtz energy is:

$$\frac{\beta A^{oa}}{V} = -\frac{\pi^2 \rho_p^2 \rho_s}{72}\sigma_s^3 [12\sigma_p^3 + 15\sigma_p^2 \sigma_s + 6\sigma_p \sigma_s^2 + \sigma_s^3] \tag{11}$$

where ρ_p and σ_p are the number density and diameter of polymer; ρ_s is the total ion density and σ_s is the mean hydrated-ion diameter.

Specific interactions are estimated from the second-order virial expansion,

$$\frac{\beta A^{ve}}{V} = \sum_i \sum_j \rho_i \rho_j B_{ij} \tag{12}$$

where B_{ij} is the osmotic second virial coefficient (with the hard-sphere contribution subtracted) for interaction between particle i and j. More accurate description requires a third order correction[68] but that is not included here.

The polyion is represented by a linear flexible chain, formed randomly from charged hard-sphere segments and neutral hard-sphere segments. To correct for connectivity between chain segments, it is necessary to include a term A^{ch} in eq. 4 for the total Helmholtz energy. As shown in Appendix B, based on our previous studies for polyelectrolyte solutions,[99-101] we can derive

$$\frac{\beta A^{ch}}{V} = \frac{1-r}{2} \rho_r \left[p_{cc} \ln y_{cc}(\sigma_c) + p_{00} \ln y_{00}(\sigma_0) + (p_{c0} + p_{0c}) \ln y_{c0}(\sigma_{c0}) \right] \tag{13}$$

where r is the polyion-chain length; ρ_r is the number density of polyion and p_{ij} is the pair probability characterizing the correlation between segments i and j. The cavity correlation function at contact, $y_{ij}(\sigma_{ij})$ is calculated from the hypernetted-chain approximation (HNC). Subscripts c and 0, respectively, represent charged segment and neutral segment.

In the McMillan-Mayer framework,[75] the chemical potential of the continuum (water) μ_0 is related to the osmotic pressure Π by

$$\mu_0 = \mu_0^{\circ} - \Pi \overline{V}_0 \tag{14}$$

where μ_0° is the chemical potential of the pure continuum and $\overline{V}_0$ is the partial volume of the continuum.

The osmotic pressure is calculated from

$$\Pi = \frac{N}{V} k_B T - \left[\frac{\partial A^{ex}}{\partial V} \right]_{T,N} \tag{15}$$

where N is the total number of molecules dissolved in the continuum.

The chemical potential of an electrically-neutral solute k is

$$\mu_k = k_B T \ln \rho_k + \mu_k^{ex} \tag{16}$$

with

$$\mu_k^{ex} = \left[\frac{\partial (A^{ex}/V)}{\partial \rho_k} \right]_{T,V,\rho_{l \neq k}} \tag{17}$$

For a charged solute k with charge Z_k (for a polyion, k now refers to the molecule after polyion-chain formation), we use the electrochemical potential[102,103]

$$\tilde{\mu}_k = \mu_k + Z_k F \Phi \tag{18}$$

where F is Faraday's constant, equal to 96487 C/equiv and Φ is the electrostatic potential relative to some reference state. In an aqueous two-phase system where the concentration of electrolyte is not the same in both phases, there is an electrostatic potential difference between the two phases.

At equilibrium, when a protein with charge Z_p partitions in an aqueous two-phase system, its electrochemical potential in one phase is identical to that in the other. From eq. 18, the partition coefficient for the protein K_p is defined by the ratio of number density in the top phase to that in the bottom phase; $K_p = \rho_p^{\mathrm{T}} / \rho_p^{\mathrm{B}}$ can be expressed as

$$\ln K_p = \ln K_p^0 + Z_p F \Delta\Phi / RT \tag{19}$$

where $\Delta\Phi$ is the electrostatic potential difference between bottom and top phases, $\Delta\Phi = \Phi^{\mathrm{B}} - \Phi^{\mathrm{T}}$; K_p^0 summarizes all contributions from the chemical potential. From eq. 16,

$$\ln K_p^0 = (\mu_p^{ex(\mathrm{B})} - \mu_p^{ex(\mathrm{T})}) / k_{\mathrm{B}} T . \tag{20}$$

K_p^0 is the partition coefficient when there is no difference of electrostatic potential ($\Delta\Phi = 0$) or when the protein is at its isoelectric point where $Z_p = 0$. Eq. 18, originally derived by Albertsson,[8] has been extensively applied to investigate the influence of electrostatic interactions on the partitioning of biomolecules.[104-106]

3. Results and Discussion

3.1 Aqueous Two-Phase-Forming Systems

In all calculations we set $T = 293\mathrm{K}$ and dielectric constant $\varepsilon_r = 78.3$, corresponding to an aqueous solution at room temperature.

We consider two typical aqueous two-phase-forming systems: a polymer/polymer system containing PEG 3000/DEX T500 and a polymer/salt system containing PEG 3000/Na_2SO_4. Accurate experimental phase diagrams are available for both systems.[71,74]

We fit the hard-sphere diameter σ_i, and single-component nonadditive parameter δ_{ii} and osmotic second virial interaction coefficient B_{ii} for polymer PEG 3000 and for DEX T500 using experimental water-activity data for binary polymer/water solutions.[71] The resulting diameter for PEG 3000 is 29.6 Å, close to 31.1 Å calculated from its hydrodynamic volume as obtained from intrinsic-viscosity data;[107] however, because an experimental diameter is available only for PEG, we cannot make a similar comparison for DEX T500. We obtain cross parameters δ_{ij} and B_{ij} from liquid-liquid equilibrium data in ternary PEG 3000/DEX T500/water solutions.[71] All parameters are shown in Tables 1-3.

Phase equilibria are calculated based on the equilibrium criteria where the osmotic pressure (equivalently, chemical potential of water) and the chemical potential for each solute in one phase must be simultaneously identical to those in the other. For an aqueous polymer/polymer system we have,

$$\Pi^{\mathrm{T}} = \Pi^{\mathrm{B}} \tag{21}$$

$$\mu_{p_1}^{\mathrm{T}} = \mu_{p_1}^{\mathrm{B}} \tag{22}$$

$$\mu_{p_2}^{\mathrm{T}} = \mu_{p_2}^{\mathrm{B}} \tag{23}$$

where superscripts T and B refer, respectively, to top phase and bottom phase; subscripts p_1 and p_2 refer, respectively, to polymer 1 and polymer 2.

Figure 1 shows the liquid-liquid phase diagram for the ternary PEG 3000/DEX T500/water system at 20 °C. Circles show experimental data[71]; the curve is calculated. Dashed and solid lines are tie lines from experiment and from this work, respectively, showing good agreement. At the critical point (or, plaint point, as it also called), shown by a triangle, the phase compositions of both phases become identical.

For a salt solution, we assume that all nonadditive parameters are zero between ions and that the osmotic second virial interaction coefficients between like ions are also zero. Using independently determined ionic diameters[108] for Na^+ (1.90 Å) and SO_4^{2-} (4.50 Å), we obtain the cross osmotic second virial interaction coefficient between Na^+ and SO_4^{2-} by fitting the literature data for osmotic coefficients of binary Na_2SO_4/water solutions.[109] Parameters for

interactions between PEG 3000 and two ions, Na^+ and SO_4^{2-}, are obtained from liquid-liquid-equilibrium data for ternary PEG 3000/ Na_2SO_4 /water solutions,[74] as shown in Tables 1-3.

If the nonadditive parameter $\delta_{ij} > 0$, there is a penetration effect between particle i and j; in contrast, there may be hydration layer between them if $\delta_{ij} < 0$. Similarly, $B_{ij} > 0$ indicates that a repulsive specific interaction exists between particle i and j; if $B_{ij} < 0$, there is an attractive specific interaction. As defined here, osmotic second virial coefficient B_{ij} is the total coefficient minus the contributions from hard-sphere repulsion and electrostatic interaction.

For an aqueous polymer/salt system, the equilibrium conditions are:

$$\Pi^{\mathrm{T}} = \Pi^{\mathrm{B}} \tag{24}$$

$$\mu_p^{\mathrm{T}} = \mu_p^{\mathrm{B}} \tag{25}$$

$$\mu_s^{\mathrm{T}} = \mu_s^{\mathrm{B}} \tag{26}$$

where subscripts p and s refer, respectively, to polymer and salt. The chemical potential of the salt is calculated from those of its ions:

$$\mu_s = (\upsilon_+\mu_+ + \upsilon_-\mu_-)/(\upsilon_+ + \upsilon_-) = (\rho_+\mu_+ + \rho_-\mu_-)/(\rho_+ + \rho_-) \tag{27}$$

where υ is a stoichiometric coefficient.

Figure 2 shows the liquid-liquid phase diagram for the ternary PEG 3000/ Na_2SO_4 /water system at 20 °C. Calculated results agree well with experiment.[74] Similar to Figure 1, the tie-line length becomes short near the critical point.

In a polymer/polymer aqueous two-phase system for protein partitioning, usually there is small amount of salt buffer in the solution. A small amount of salt does not affect the phase equilibria; however, because unequal partitioning of the salt may cause a difference in electrostatic potential between the two phases, a buffer salt may exert a major influence on the partitioning behavior of a charged protein.[66,84]

Using the parameters discussed above and those between DEX T500 and Na_2SO_4,[87,88] we calculate phase equilibria for the PEG 3000/DEX T500 aqueous system containing 0.01M Na_2SO_4. The equilibrium conditions are eqs. (21-23) and (26). The phase diagram is essentially identical to that without Na_2SO_4 shown in Figure 1. However, the salt is unequally distributed;

its concentration in the DEX-rich phase (bottom) is larger than that in the PEG-rich phase (top). Due to this unequal distribution of salt, there is an electrostatic potential difference $\Delta\Phi$ between both phases, which is estimated by [8,110]

$$\Delta\Phi = \frac{RT}{(Z_+ - Z_-)F} \ln \frac{K_-}{K_+} \tag{28}$$

where $K_+ = \rho_+^{\mathrm{T}} / \rho_+^{\mathrm{B}}$ and $K_- = \rho_-^{\mathrm{T}} / \rho_-^{\mathrm{B}}$, respectively, denote partition coefficients of cation and anion. Here $\Delta\Phi = \Phi^{\mathrm{B}} - \Phi^{\mathrm{T}}$.

Figure 3 shows the partitioning coefficient of salt as a function of tie-line length, along with the calculated electrostatic potential difference in the PEG 3000/DEX T500 aqueous two-phase system containing 0.01M Na_2SO_4.

Figure 4 shows the calculated electrostatic potential difference as a function of tie-line length in the PEG 3000/ Na_2SO_4 aqueous two-phase system.

It is not simple to obtain an unambiguous measurement of $\Delta\Phi$. Our calculated results are consistent with the common knowledge[111] that the electrostatic potential difference in aqueous two-phase systems is in the range 0~10 mV.

3.2 Native Protein Partitioning

In typical cases, protein concentrations in the aqueous solutions are approximately or less than 0.001 g/g; such small concentrations of partitioning biomolecules do not change the compositions of the phase-forming components beyond the limits of experimental uncertainty.[38] Therefore, for very dilute protein solutions, we assume that there is no effect of protein concentration on the equilibrium distributions of polymers and ions in the aqueous two-phase systems described above.

Partitioning of native proteins in aqueous two-phase systems, as introduced in Sec.1, has been extensively investigated.[54,61-63,66-68,84,87,88] Here, we present a calculation for the partitioning of a typical native protein, lysozyme, with diameter 30 Å [112] and positive charge 7 (at pH 7). Using parameters in Tables 1-3 and those in Table 4 for interactions between lysozyme and polymers, and ions,[84,87,88] we calculate the partition coefficients of lysozyme in the aqueous PEG 3000/DEX T500 system with 0.01M Na_2SO_4. At equilibrium, the electrochemical potential of the protein in the top phase is equal to that in the bottom phase, i.e., $\tilde{\mu}_p^{\mathrm{T}} = \tilde{\mu}_p^{\mathrm{B}}$. Results are shown

in Figure 5. For the partitioning of lysozyme in the aqueous PEG 3000/ Na_2SO_4 system, similar results are shown in Figure 6.

If $\Delta\Phi = 0$, $K_p = K_p^0$. In that event, lysozyme favors the top PEG-rich phase; however, accounting for the electrostatic potential difference, $K_p < K_p^0$ and lysozyme favors the bottom DEX-rich phase.

Protein charge depends on pH. If the protein is negatively charged, from eq (19), $K_p > K_p^0$. In that event, partitioning into the top phase is enhanced.

3.3 Denatured Protein Partitioning

In our polyion model for a denatured (linear) protein, we assume that the diameter of a charged segment is identical to that of a neutral segment, equal to 3.0 Å; each charged segment carries unit positive charge. Nonadditive parameters between all segments and polymers are 0.02. If we further set the polyion chain length $r = 1000$ and charge fraction $f = 0.007$, this polyion chain can be mapped to the above-discussed native protein with diameter 30 Å and positive charge 7; both proteins occupy the same volume and carry the same charge.

Given osmotic second virial interaction coefficients shown in Table 4 for characterizing specific interactions between the segments of the polyion and the phase-forming polymers and ions, we calculate partition coefficients for some polyion model systems to represent partition coefficients for denatured proteins in aqueous two-phase systems.

Figure 7(a) shows calculated partition coefficients for short polyion chains $r = 2, 4$ and 6 in the PEG 3000/DEX T500/0.01M Na_2SO_4 aqueous two-phase system. The charge fraction for each chain is very small with $f = 0.007$. Figure 7(b) shows experimental data for short tryptophan peptides partitioning in the aqueous PEG 6000/DEX T500/0.01M potassium phosphate system with the assumption that peptides carry no charge at pH = 6.[47] Circles, triangles and squares are, respectively, for tryptophan, di-tryptophan and tri-tryptophan. Lines are drawn to guide the eye. Although we cannot directly compare our calculations with experiment, our model gives the same trends as those measured. As chain length rises, the partition coefficient becomes large because the area of contact between protein and phase-forming components increases. Because the charge fraction is small, from eq 19, the effect of electrostatic potential difference is negligible.

Figure 8 shows partition coefficients for model polyions with long chain lengths in aqueous PEG 3000/DEX T500/0.01M Na_2SO_4. From bottom to top, $r=2$, 4, 6, 100, 1000. As chain length r rises, $\ln K$ increases in proportion to r. The denatured protein partitions strongly into the top phase consistent with the experimental observation[8] that, while a biomolecule with low molecular weight partitions nearly equally between two phases, as molecular weight rises, the partition coefficient rapidly deviates from unity. For some large linear biomolecules such as DNA, or for a virus with a very large molecular weight, partition into one phase becomes complete.

For a mixture containing native protein (diameter 30Å and positive charge 7) and a corresponding denatured protein (segment diameter 3.0Å, chain length $r=1000$ and charge fraction $f=0.007$), we find that while the native protein favors the bottom phase, the denatured protein partitions completely to the top phase. Therefore, an aqueous two-phase system provides a suitable method for separating otherwise similar native and denatured proteins.

Figure 9(a) shows calculated partition coefficients for short polyion chains $r=2,4$ and 6 in the aqueous PEG 3000/Na_2SO_4 system with charge fraction $f=0.007$. Figure 9(b) shows experimental data for short tryptophan peptides partitioning in the aqueous PEG 6000/Na_2SO_4 system at pH$=6$.[46,47] For this aqueous polymer/salt system, our calculations and experiment show the same trend, similar to that shown in an aqueous polymer/polymer system.

Figure 10, similar to Figure 8, shows partition coefficients for model polyions with long chain lengths in the aqueous PEG 3000/Na_2SO_4 system; from bottom to top, $r=2$, 4, 6, 100, 1000.

4. Conclusion

Within the McMillan-Mayer solution theory, we have established a molecular-thermodynamic theory for partitioning of native and denatured proteins in aqueous two-phase systems. Interactions between solute molecules are accounted for through potential of mean force in a continuous medium (water).

To illustrate application, we have calculated phase diagrams for the aqueous polymer/polymer phase-forming system PEG 3000/DEX T500 with or without salt buffer and for the aqueous polymer/salt system PEG 3000/Na_2SO_4. Good agreement with experiment is obtained. Because

salt distributes unequally between the two phases, there is an electrostatic potential difference that can have a major influence on protein partitioning if the protein carries charge.

The partitioning behavior of a native protein is quite different from that of a denatured protein.[38,113] Native protein has a compact conformation where most protein segments are buried inside; however, when a native protein denatures, these segment are exposed into the medium. As a result, there is increased interaction between protein segments and other components in the solution, producing more asymmetric partitioning. As the protein denatures more, the number of exposed segments rises, causing increased change in partitioning behavior.

The theory developed here may be useful also for describing partitioning of combination peptides,[44,45] and of protein-peptide fusion tags[114-116] in aqueous two-phase systems.

Acknowledgment. We thank Dr. Christian Rämsch and Prof. M.-R. Kula (Institute of Enzymetechnology, Heinrich-Heine Universität Düsseldorf, Jülich) for helpful discussions and for providing the data shown in Figures 7(b) and 9(b). This work was supported by the Director, Office of Science, Office of Basic Energy Sciences, Chemical Sciences Division of the U.S. Department of Energy under Contract Number DE-AC03-76SF00098. Additional support was given by the National Science Foundation and by the Chinese National Science Foundation.

Appendix A. Osmotic Attraction

From Asakura and Oosawa,[93,94] the short-range osmotic attraction potential between polymer particles in a polymer/salt solution is:

$$\beta W^{oa}(R) = \begin{cases} -\dfrac{4\pi}{3}\rho_s\sigma_{ps}^3\left[1-\dfrac{3R}{4\sigma_{ps}}+\dfrac{R^3}{16\sigma_{ps}^3}\right] & \sigma_p \le R \le 2\sigma_{ps} \\ 0 & R > 2\sigma_{ps} \end{cases} \tag{A.1}$$

where R is the center-center distance; ρ_s is the total ion density; $\sigma_{ps} = (\sigma_p + \sigma_s)/2$; σ_p is the polymer diameter and σ_s is the mean hydrated ion diameter.

Using the random-phase approximation where all correlations between particles in the domain of attractive potential are neglected,

$$\frac{\beta A^{oa}}{V} = \frac{1}{2}\rho_p^2 \int \beta W^{oa}(R) 4\pi R^2 \mathrm{d}R \tag{A.2}$$

where ρ_p is the number density of polymer. Integration gives

$$\frac{\beta A^{oa}}{V} = -\frac{\pi^2 \rho_p^2 \rho_s}{72}\sigma_s^3[12\sigma_p^3 + 15\sigma_p^2\sigma_s + 6\sigma_p\sigma_s^2 + \sigma_s^3]. \tag{A.3}$$

Osmotic attraction exists also between protein particles in an aqueous polymer/salt system. However, because the protein concentration is assumed to be very small, this contribution is negligible.

Appendix B. Polyion with Randomly Distributed Charged Hard Spheres and Neutral Hard Spheres

The polyion is represented by a freely tangent-joined, linear, flexible chain with length r. Charged hard-sphere segments and neutral hard-sphere segments are randomly distributed along the polyion chain; the average mole fraction of charged hard-sphere segments is f. We assume a blockiness parameter θ to characterize the sequence, i.e., the strength of chemical correlations along the chain. Then, the pair probabilities are

$$p_{cc} = f(1-\theta)+\theta \tag{B.1}$$

$$p_{00} = f(\theta-1)+1 \tag{B.2}$$

$$p_{c0} = 1 - p_{00} \tag{B.3}$$

$$p_{0c} = 1 - p_{cc} \tag{B.4}$$

where subscripts c and 0, respectively, represent charged segment and neutral segment.

With these equations, we can derive the contribution to the Helmholtz energy due to formation of a polyion chain:

$$\frac{\beta A^{ch}}{V} = \frac{1-r}{2}\rho_r\left[p_{cc}\ln y_{cc}(\sigma_c) + p_{00}\ln y_{00}(\sigma_0) + (p_{c0} + p_{0c})\ln y_{c0}(\sigma_{c0})\right]. \tag{B.5}$$

In our calculations, we set $\theta = 0$ denoting that the distribution of charged and neutral segments is random.

References and Notes

(1) Beijerinck, M. W. *Zbl. Bakt.* **1896**, *2*, 697.

(2) Albertsson, P.-Å. *Nature* **1956**, *177*, 771.

(3) Albertsson, P.-Å. *Nature* **1958**, *182*, 709; *Biochim. Biophys. Acta* **1958**, *27*, 378.

(4) Kula, M.-R. In *Appl. Biochem. Bioeng.*; Wingard, L. B. Jr.; Katchalski-Katzir, E.; Goldstein, L., Eds.; Academic Press: New York, p.71, 1979.

(5) Kula, M.-R.; Kroner, K. H.; Hüstedt, H. *Adv. Biochem. Eng.* **1982**, *24*, 73.

(6) Walter, H.; Brooks, D. E.; Fisher, D. *Partitioning in Aqueous Two-Phase Systems: Theory, Methods, Uses, and Applications to Biotechnology*; Academic Press: Orlando, FL, 1985.

(7) Abbott, N. L.; Hatton, T. A. *Liquid-Liquid Extraction for Protein Separation*; MIT: Cambridge, MA, 1988.

(8) Albertsson, P.-Å. *Partition of Cell Particles and Macromolecules*, 3rd Ed.; Wiley-Interscience: New York, 1986.

(9) Albertsson, P.-Å.; Johansson, G.; Tjerneld, F. In *Separation Processes in Biotechnology*; Asenjo, J. A., Ed.; Marcel Dekker: New York, p.287, 1990.

(10) Raghavarao, K. S. M. S.; Guinn, M. R.; Todd, P. *Sep. Purif. Methods* **1998**, *27*, 1.

(11) Hansson, U.-B.; Wingren, C. *Sep. Purif. Methods* **1998**, *27*, 169.

(12) Mattiasson, B; Mandenius, C. F.; Axelsson, J. P.; Danielsson, B.; Hagander, P. *Annals New York Acad. Sci.* **1983**, *413*, 193.

(13) Shanbhag, V. P.; Axelsson, *Eur. J. Biochem.* **1975**, *60*, 17.

(14) Zaslavsky, B. Yu.; Miheeva, L. M.; Mestechkina, N. M.; Rogozhin, S. V. *J. Chromatogr.* **1982**, *253*, 139, 149; **1983**, *256*, 49.

(15) Shanbhag, V. P.; Sodergard, R.; Carstensen, H.; Albertsson, P.-Å. *J. Steroid Biochem.* **1973**, *4*, 537.

(16) Ling, T. G.; Mattiasson, B. *J. Chromatogr.* **1982**, *252*, 159.

(17) Mattiasson, B. *Methods. in Enzym.* **1983**, *92*, 498.

(18) Carlsson, M.; Linse, P.; Tjerneld, F. *Macromol.* **1993**, *26*, 1546.

(19) Zhangm K.; Carlsson, M.; Linse, P.; Lindman, B. *J. Phys. Chem.* **1994**, *98*, 2452.

(20) Hamad, E. Z.; Ijaz, W.; Ali, S. A.; Hastaoglu, M. A. *Biotech. Prog.* **1996**, *12*, 173.

(21) Li, M.; Zhu, Z.-Q.; Mei, L.-H. *Biotech. Prog.* **1997**, *13*, 105.

(22) Li, M.; Wang, Y.-X.; Zhu, Z.-Q. *J. Chem. Eng. Data* **1998**, *43*, 93.

(23) Jönsson, B.; Lindman, B.; Holmberg, K.; Kronberg, B. *Surfactants and Polymers in Aqueous Solution*; Jone Wiley & Sons: New York, 1998.

(24) Piculell, L.; Lindman, B. *Adv. Colloid Interface Sci.* **1992**, *41*, 149.

(25) Sivars, U.; Bergfeldt, K.; Piculell, L.; Tjerneld, F. *J. Chromatogr.* B **1996**, *680*, 43.

(26) Nikas, Y. J., Liu, C.-L.; Srivastava, T.; Abbott, N. L.; Blankschtein, D. *Macromolecules* **1992**, *25*, 4794.

(27) Liu, C.-L.; Nikas, Y. J.; Blankschtein, D. *AIChE J.* **1995**, *41*, 991.

(28) Liu, C.-L.; Nikas, Y. J.; Blankschtein, D. *Biotech. Bioeng.* **1996**, *52*, 185.

(29) Albertsson, P.-Å.; Cajarville, A.; Brooks, D. E.; Tjerneld, F. *Biochim. Biophys. Acta* **1987**, *926*, 87.

(30) Forciniti, D.; Hall, C. K.; Kula, M.-R. *Fluid Phase Equil.* **1991**, *61*, 243; *AIChE J.* **1991**, *38*, 986.

(31) Kroner, K. H.; Kula, M.-R. *Proc. Biochem.* **1978**, April, 7.

(32) Hustedt, H.; Kroner, K. H.; Stach, W.; Kula, M.-R. *Biotech. Bioeng.* **1978**, *XX*, 1988.

(33) Hustedt, H.; Johansson, G.; Tjerneld, F. *Bioseparation* **1990**, *1*, 177.

(34) Asenjo, J. A.; Schmidt, A. S.; Hachem, F.; Andrews, B. A. *J. Chromatogr.* A **1994**, *668*, 47.

(35) Zaslavsky, D. Y. *Aqueous Two-Phase Partitioning: Physical Chemistry and Bioanalytical Applications*; Marcel Dekker: New York, 1995.

(36) Albertsson, P.-Å. *Arch. Biochem. Biophys. Suppl.* **1962**, *1*, 264.

(37) Albertsson, P.-Å. *Biochim. Biophys. Acta* **1965**, *103*, 1.

(38) Albertsson, P.-Å. *Adv. Protein Chem.* **1970**, *24*, 309.

(39) Pettijohn, D. E. *Eur. J. Biochem.* **1967**, *3*, 25; 33.

(40) Pettijohn, D. E. In *Progress in Separation and Purification,* Vol. II, Gerritsen, T., Ed.; Wiley-Interscience: New York, p.147, 1969.

(41) Kang, E.-C.; Akiyoshi, K.; Sunamoto, J. *J. Bioact. Comp. Polym.* **1999**, *14*, 6.

(42) Großmann, G.; Tintinger, R.; Zhu, J.; Maurer, G. *Fluid Phase Equil.* **1997**, *137*, 209.

(43) Tintinger, R.; Zhu, J.; Großmann, G.; Maurer, G. *J. Chem. Eng. Data* **1997**, *42*, 975.

(44) Tintinger, R.; Zhu, J.; Großmann, G.; Maurer, G. *Ber. Bunsenges. Phys. Chem.* **1997**, *101*, 687.

(45) Großmann, G.; Tintinger, R.; Zhu, J.; Maurer, G. *Biotech. Bioeng.* **1998**, *60*, 699.

(46) Rämsch, C.; Kleinelanghorst, L. B.; Knieps, E. A.; Thömmes, J.; Kula, M.-R. *Biotech. Prog.* **1999**, *15*, 493.

(47) Rämsch, C.; Kleinelanghorst, L. B.; Knieps, E. A.; Thömmes, J.; Kula, M.-R. *Biotech. Bioeng.* in press.

(48) Abbott, N. L.; Blankschtein, D.; Hatton, T. A. *Bioseparation* **1990**, *1*, 191.

(49) Walter, H.; Johansson, G.; Brooks, D. E. *Anal. Biochem.* **1986**, *155*, 215; **1991**, *197*, 1.

(50) Cabezas Jr., H. *J. Chromatogr. B* **1996**, *680*, 3 and references therein.

(51) Brooks, D. E.; Sharp, K. A.; Fisher, D. In *Partitioning in Aqueous Two-Phase Systems: Theory, Methods, Uses, and Applications to Biotechnology*; Walter, H.; Brooks, D. E.; Fisher, D., Eds.; Academic Press: Orlando, FL, 1985.

(52) Gustafsson, A.; Wennerström, H.; Tjerneld, F. *Polymer*, **1986**, *27*, 1768; *Fluid Phase Equil.* **1986**, *29*, 365.

(53) Flory, P. J. *J. Chem. Phys.* **1942**, *10*, 51; Huggins, M. L. *J. Phys. Chem.* **1942**, *46*, 151.

(54) Diamond, A. D.; Hsu, J. T. *Biotech. Bioeng.* **1989**, *34*, 1000; *AIChE J.* **1990**, *36*, 1017.

(55) Hino, T.; Prausnitz, J. M. *J. Appl. Polym. Sci.* **1998**, *68*, 2007.

(56) Scheutjens, J. M. H. M.; Fleer, G. *J. Phys. Chem.* **1979**, *83*, 1619; **1980**, *84*, 178.

(57) Baskir, J.; Hatton, T. A.; Suter, U. W. *Macromol.* **1987**, *20*, 1300; *Biotech. Bioeng.* **1989**, *34*, 541; *J. Phys. Chem.* **1989**, *93*, 2111.

(58) Pizter, K. S.; Li, Y. *Proc. Natl. Acad. Sci. U. S.* **1983**, *80*, 7689.

(59) Peng, Q.; Li, Z.; Li Y. *Fluid Phase Equil.* **1995**, *107*, 303.

(60) de Gennes, P. G. Scaling *Concepts in Polymer Physics*; Cornell University Press: Ithaca, 1979.

(61) Abbott, N. L.; Blankschtein, D.; Hatton, T. A. *Macromol.* **1991**, *24*, 4334; **1992**, *25*, 3917, 3932, 5192; **1993**, *26*, 825.

(62) Abbott, N. L.; Blankschtein, D.; Hatton, T. A. In *Colloid-Polymer Interactions: Particulate, Amphiphilic and Biological Surfaces*, Dubin, P. L.; Tong, P., Ed.; ACS Symp. Ser. 532, San Francisco, April 1992.

(63) Kilpatrick, P. K. *Am. Sci.* **1995**, *83*, 95.

(64) Edmond, E.; Ogston, A. *Biochem. J.* **1968**, *109*, 569; **1970**, *117*, 85.

(65) Harding, S. E.; Horton, J. C.; Jones, S.; et al. *Biophysical J.* **1999**, *76*, 2432.

(66) King, R. S.; Blanch, H. W.; Prausnitz, J. M. *AIChE J.* **1988**, *34*, 1585.

(67) Haynes, C. A.; Blanch, H. W.; Prausnitz, J. M. *Fluid Phase Equil.* **1989**, *53*, 463.

(68) Haynes, C. A.; Beynon, R. A.; King, R. S.; Blanch, H. W.; Prausnitz, J. M. *J. Phys. Chem.* **1989**, *93*, 5612.

(69) Zhou, F.; Kakisaka, K.; Ishidao, T.; Iwai, Y.; Arai, Y.; Furuya, T. *J. Chem. Eng. Japan* **1997**, *30*, 349; **1998**, *31*, 991.

(70) Wu, Y.-T.; Lin, D.-Q.; Zhu, Z.-Q.; Mei, L.-H. *Fluid Phase Equil.* **1996**, *124*, 67.

(71) Gaube, J.; Pfennig A.; Stumpf, M. *J. Chem. Eng. Data* **1991**, *36*, 446; **1993**, *38*, 163, 207.

(72) Gaube, J.; Pfennig A.; Stumpf, M. *Fluid Phase Equil.* **1993**, *83*, 365.

(73) Döbert, F.; Pfennig A.; Stumpf, M. *Macromol.* **1995**, *28*, 7860.

(74) Hammer, S.; Pfennig, A.; Stumpf, M. *J. Chem. Eng. Data*, **1994**, *39*. 409.

(75) McMillan Jr., W. G.; Mayer, J. E. *J. Chem. Phys.* **1945**, *13*, 276.

(76) Hill, T. L. *Introduction to Statistical Mechanics*, Addison-Wesley: Reading, MA, 1986.

(77) Cabezas Jr., H.; Evans, J. D.; Szlag, D. C. *Fluid Phase Equil.* **1989**, *53*, 453.

(78) Cabezas Jr., H.; Evans, J. D.; Szlag, D. C.; In *Downstream Processing and Bioseparation*, Hamel, J. F. et al., Eds.; ACS Symp. Ser. 419; American Chemical Society, Washington, DC, 1990.

(79) Kabiri-Badr, M.; Cabezas Jr., H. *Fluid Phase Equil.* **1996**, *115*, 39.

(80) Forciniti, D.; Hall, C. K.; In *Downstream Processing and Bioseparation*, Hamel, J. F. et al., Eds.; ACS Symp. Ser. 419; American Chemical Society, Washington, DC, 1990.

(81) Kang, C.; Sandler, S. I. *Fluid Phase Equil.* **1987**, *38*, 245; *Biotech. Bioeng.* **1988**, *32*, 1158; *Macromol.* **1988**, *21*, 3088.

(82) Abram, D. S.; Prausnitz, J. M. *AIChE J.* **1975**, *21*, 116.

(83) Guggenheim, E. A. *Philos. Mag. Ser. 7* **1935**, *19*, 588; *Trans. Faraday Soc.* **1966**, *62*, 3446.

(84) Hartounian, H.; Sandler, S. I; Kaler, E. W. *Ind. Eng. Chem. Res.* **1994**, *33*, 2288, 2294.

(85) Fredenslund, A.; Gmehling, J.; Rasmussen, P. *Vapor-Liquid Equilibria Using UNIFAC, A Group Contribution Method*, Elsevier Scientific: New York, 1977.

(86) Peng, Q.; Li, Z.; Li Y. *Fluid Phase Equil.* **1994**, *95*, 341.

(87) Haynes, C. A. *Separation of Protein Mixtures by Extraction*; PhD Thesis; University of California, Berkeley, CA, 1992.

(88) Haynes, C. A.; Benitez, F. J.; Blanch, H. W.; Prausnitz, J. M. *AIChE J.* **1993**, *39*, 1539.

(89) Kenkare, P. U; Hall, C. K. *AIChE J.* **1996**, *42*, 3508.

(90) Georgalis, Y.; Zouni, A.; Eberstein, W.; Saenger, W.; *J. Cryst. Growth* **1993**, *126*, 245.

(91) Kuehner, D. E; Heyer, C.; Rämsch, C.; Fornefeld, U. M.; Blanch, H. W.; Prausnitz, J. M. *Biophys. J.* **1997**, *73*, 3211.

(92) Curtis, R. A.; Prausnitz, J. M.; Blanch, H. W. *Biotech. Bioeng.* **1998**, *57*, 11.

(93) Asakura,T.; Oosawa, F. *J. Chem. Phys.* **1954**, *22*, 1255.

(94) Asakura,T.; Oosawa, F. *J. Polym. Sci.* **1958**, *33*, 183.

(95) Winzor, D. J.; Wills, P. R. In *Protein-Solvent Interactions*, Gregory, R. B., Ed.; Marcel Dekker: New York, 1995.

(96) Boublik, T. *J. Chem. Phys.* **1990**, *53*, 471; Mansoori, G. A.; Carnahan, N. F.; Starling, K. E.; Leland, T. W. *ibid.* **1971**, *54*, 1523.

(97) Harvey, A. H. *Molecular-Thermodynamics of Mixtures Containing Electrolytes with Common Gases and Solvents*; PhD Thesis; University of California, Berkeley, CA, 1988. Harvey, A. H.; Prausnitz, J. M. *Fluid Phase Equil.* **1989**, *48*, 197.

(98) Blum, L. *Mol. Phys.* **1975**, *30*, 1529; Blum L.; Hoye J. S. *J. Phys. Chem.*, **1977**, *81*, 1311.

(99) Jiang, J.; Liu, H.; Hu Y.; Prausnitz, J. M. *J. Chem. Phys.* **1998**, *108*, 780.

(100) Jiang, J.; Liu, H.; Hu Y. *J. Chem. Phys.* **1999**, *110*, 4952.

(101) Jiang, J.; Prausnitz, J. M. *J. Phys. Chem. B* **1999**, *103*, 5560.

(102) Haynes, C. A.; Carson, J.; Blanch, H. W.; Prausnitz, J. M. *AIChE J.* **1991**, *37*, 1401.

(103) Newman, J. *Electrochemical Systems*, 2nd Ed.; Prentice Hall: New Jersey, 1991.

(104) Schluck, A.; Maurer, G.; Kula, M.-R. *Biotech. Bioeng.* **1995**, *46*, 443; *47*, 252.

(105) Luther, J. R.; Glatz, C. E.; *Biotech. Bioeng.* **1994**, *44*, 147; **1995**, *46*, 62.

(106) Fan, W.; Bakir, U.; Glatz, C. E.; *Biotech. Bioeng.* **1998**, *59*, 461.

(107) Atha, D. H.; Ingham, K. C. *J. Bio. Chem.* **1981**, *256*, 12108.

(108) Marcus, Y. *J. Sol. Chem.* **1983**, *12*, 271.

(109) Robinson, R. A.; Stokes, R. H. *Electrolyte Solutions*, 3rd Ed.; Butterworths Scientific Publications: London, 1970.

(110) Pfennig, A.; Schwerin, A. *Fluid Phase Equil.* **1995**, *108*, 305; *Ind. Eng. Chem. Res.* **1998**, *37*, 3180; *J. Chromatogr. B*, **1998**, *711*, 45.

(111) Reitherman, R.; Flanagan, S. D.; Barondes, S. H. *Biochim. Biophys. Acta* **1973**, *297*, 193.

(112) Tyn, M. T.; Gusek, T. W. *Biotech. Bioeng.* **1990**, *35*, 327.

(113) Viñograd, J.; Lebowitz, J.; Rodloff, R.; Watson, R.; Laipis, P. *Proc. Natl. Acad. Sci. U. S.* **1965**, *53*, 1104.

(114) Eiteman, M. A.; Hassinen, C.; Veide, A. *Biotech. Prog.* **1994**, *10*, 513.

(115) Carlsson, M.; Berggren, K.; Linse, P.; Veide, A.; Tjerneld, F. *J. Chromatogr. A* **1996**, *756*, 107.

(116) Berggren, K.; Veide, A.; Nygren, P.-Å.; Tjerneld, F. *Biotech. Bioeng.* **1999**, *62*, 135.

TABLE 1: Molecular Weights M_w and Hard-Sphere Diameters σ_i for PEG 3000, DEX T500 and Na_2SO_4

Polymer or Salt	M_w (g/mol)	σ(Å)
PEG 3000	2840[a]	29.6
DEX T500	101000[a]	149.4
Na^+	23	1.90
SO_4^{2-}	96	4.50

[a] number-average molecular weight.

TABLE 2: Nonadditive Parameters δ_{ij} for PEG 3000, DEX T500 and Na_2SO_4

Polymer or Salt	PEG 3000	DEX T500	Na^+	SO_4^{2-}
PEG 3000	0.020	−0.014	−0.077	−0.019
DEX T500	−0.014	0.012	0.05	0.05
Na^+	−0.077	0.05	0	0
SO_4^{2-}	−0.019	0.05	0	0

TABLE 3: Perturbation Contributions to the Osmotic Second Virial Coefficients B_{ij} (L/mol) for PEG 3000, DEX T500 and Na_2SO_4

Polymer or Salt	PEG 3000	DEX T500	Na^+	SO_4^{2-}
PEG 3000	−1.25	−8.24	0.086	−4.01
DEX T500	−8.24	−62.5	−88.9	−1481
Na^+	0.086	−88.9	0	−0.09
SO_4^{2-}	−4.01	−1481	−0.09	0

TABLE 4: Perturbation Contributions to the Osmotic Second Virial Coefficients B_{ij} (L/mol) for Native and Denatured Proteins with PEG 3000, DEX T500 and Na_2SO_4

Polymer or Salt	Native Protein	Denatured Protein	
		Charged Segment	Neutral Segment
PEG 3000	–6.34	–70	–70
DEX T500	–785	–1000	–1000
Na^+	0	0	–5.5
SO_4^{2-}	–3.08	10	10

Figure 1. Phase diagram for the PEG 3000/DEX T500 aqueous two-phase system. Circles: experimental data.[71] Curve: calculated results of this work. Dashed line: experimental tie line;[71] solid line: calculated tie line of this work. Solid triangle: critical point.

Figure 2. Phase diagram for the PEG 3000/Na_2SO_4 aqueous two-phase system. Circles: experimental data.[74] Curve: calculated results of this work. Dashed line: experimental tie line;[74] solid line: calculated tie line of this work. Solid triangle: critical point.

Figure 3. Salt partition coefficient and calculated electrostatic potential difference in the PEG 3000/DEX T500 aqueous two-phase system with 0.01M Na_2SO_4.

Figure 4. Calculated electrostatic potential difference in the PEG 3000/Na_2SO_4 aqueous two-phase system.

Figure 5. Native protein lysozyme partition coefficient in the PEG 3000/DEX T500 aqueous two-phase system with 0.01M Na_2SO_4.

Figure 6. Native protein lysozyme partition coefficient in the PEG 3000/Na_2SO_4 aqueous two-phase system.

Figure 7. (a) Partition coefficients for short peptides in the PEG 3000/DEX T500 aqueous two-phase system with 0.01M Na_2SO_4. (b) Experimental data:[47] Circles for tryptophan; triangles for di-tryptophan; squares for tri-tryptophan. Lines are drawn to guide the eye.

Figure 8. Partition coefficients for denatured proteins with various chain lengths in the PEG 3000/DEX T500 aqueous two-phase system with 0.01M Na_2SO_4. From bottom to top, $r = 2$, 4, 6, 100, 1000.

Figure 9. (a) Partition coefficients for short peptides in the PEG 3000/Na_2SO_4 aqueous two-phase system. (b) Experimental data:[47] Circles for tryptophan; triangles for di-tryptophan; squares for tri-tryptophan. Lines are drawn to guide the eye.

Figure 10. Partition coefficients for denatured proteins with various chain lengths in the PEG 3000/Na_2SO_4 aqueous two-phase system. From bottom to top, $r = 2$, 4, 6, 100, 1000.

Fig.1

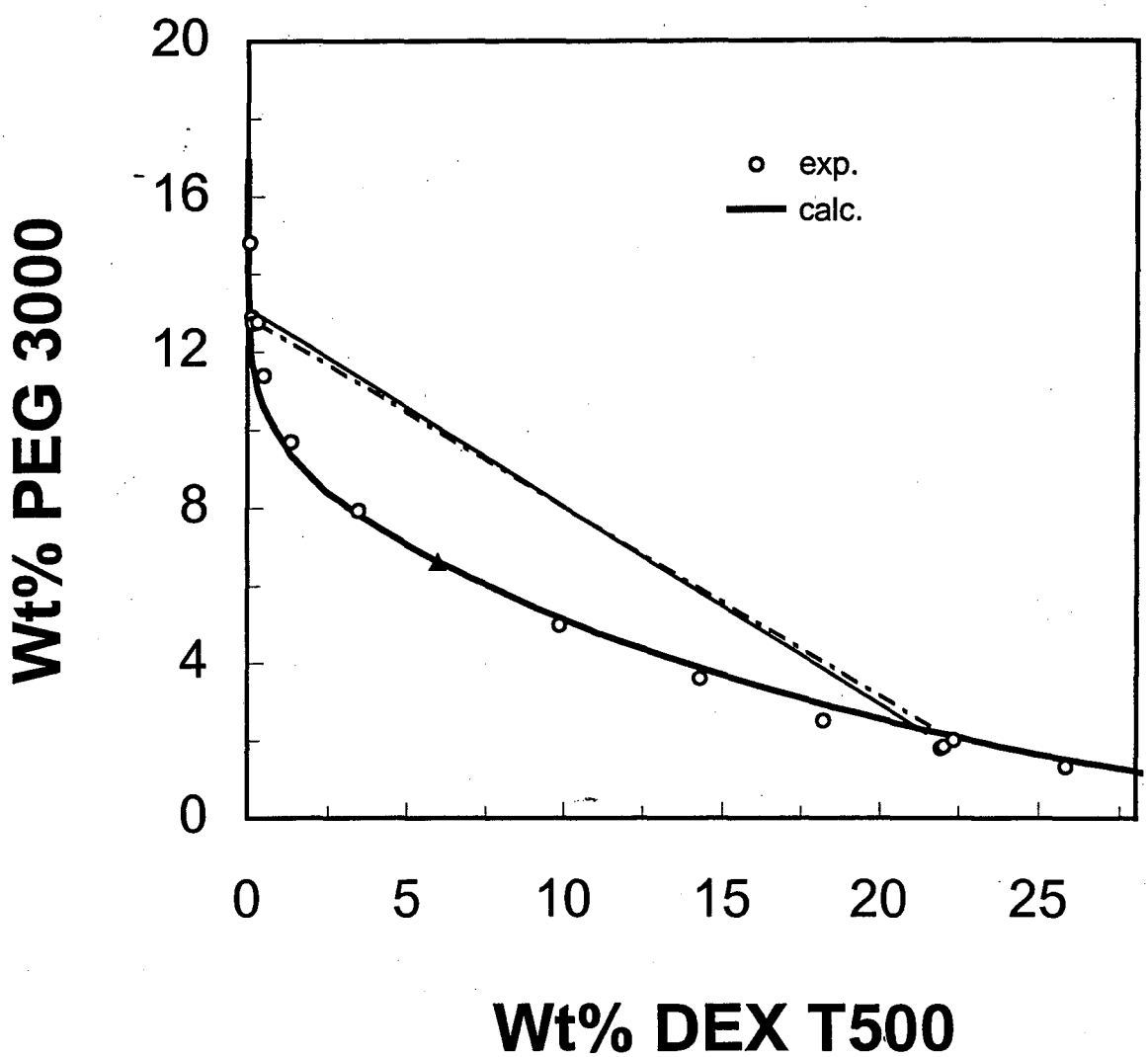

Fig

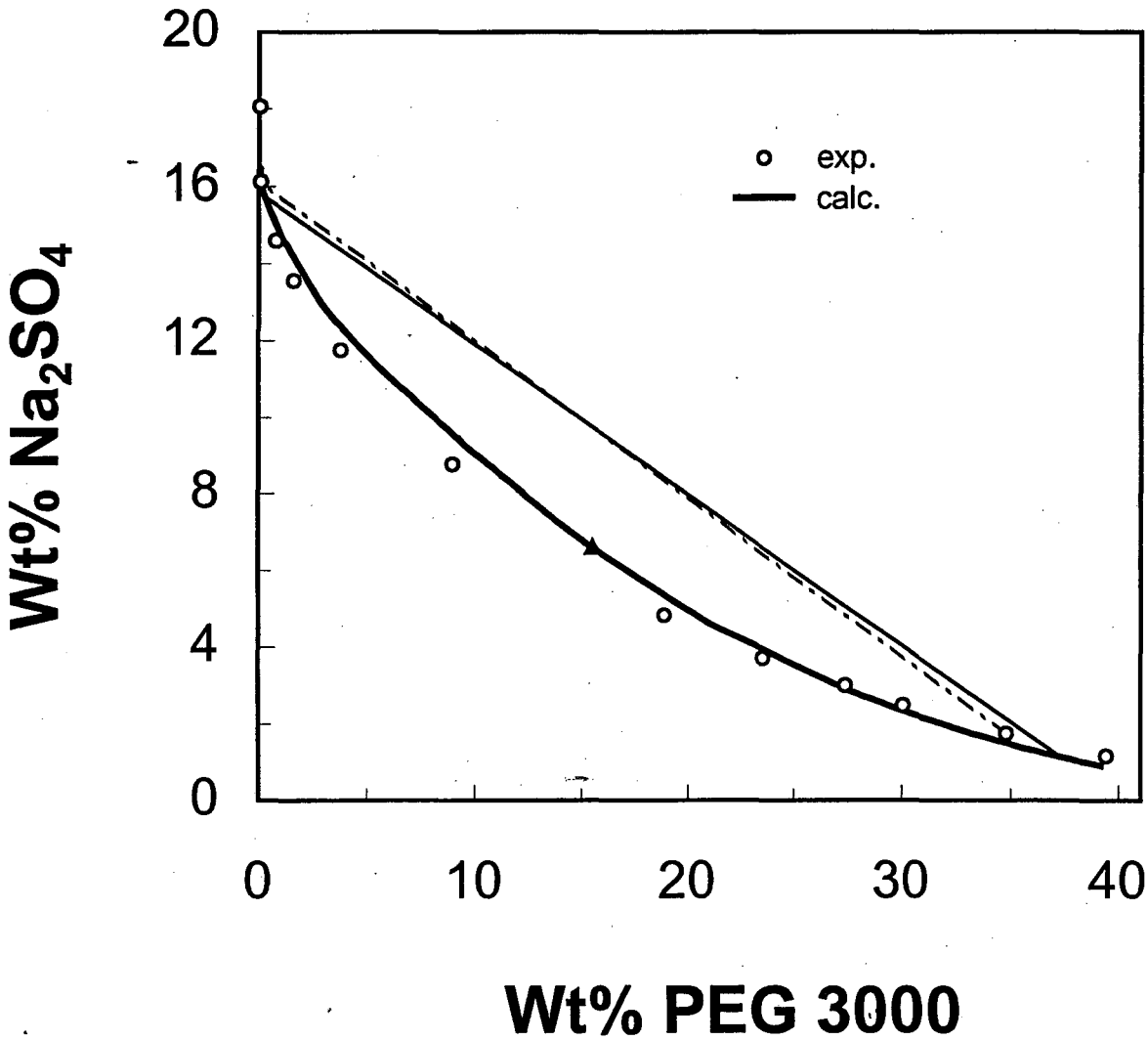

Fig.3

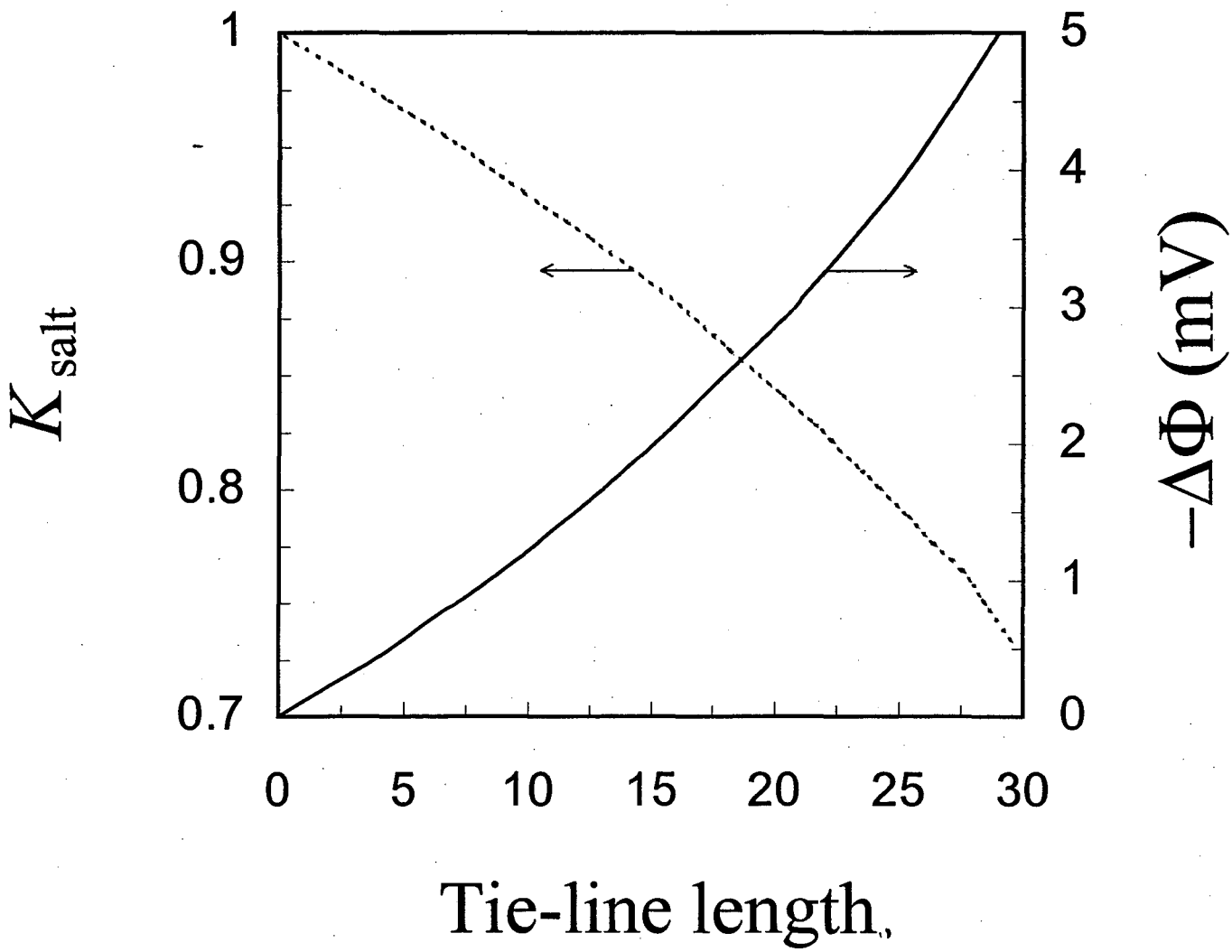
1
0.9
0.8
0.7
K_{salt}
5
4
3
2
1
0
$-\Delta\Phi$ (mV)
0
5
10
15
20
25
30
Tie-line length

Fig.

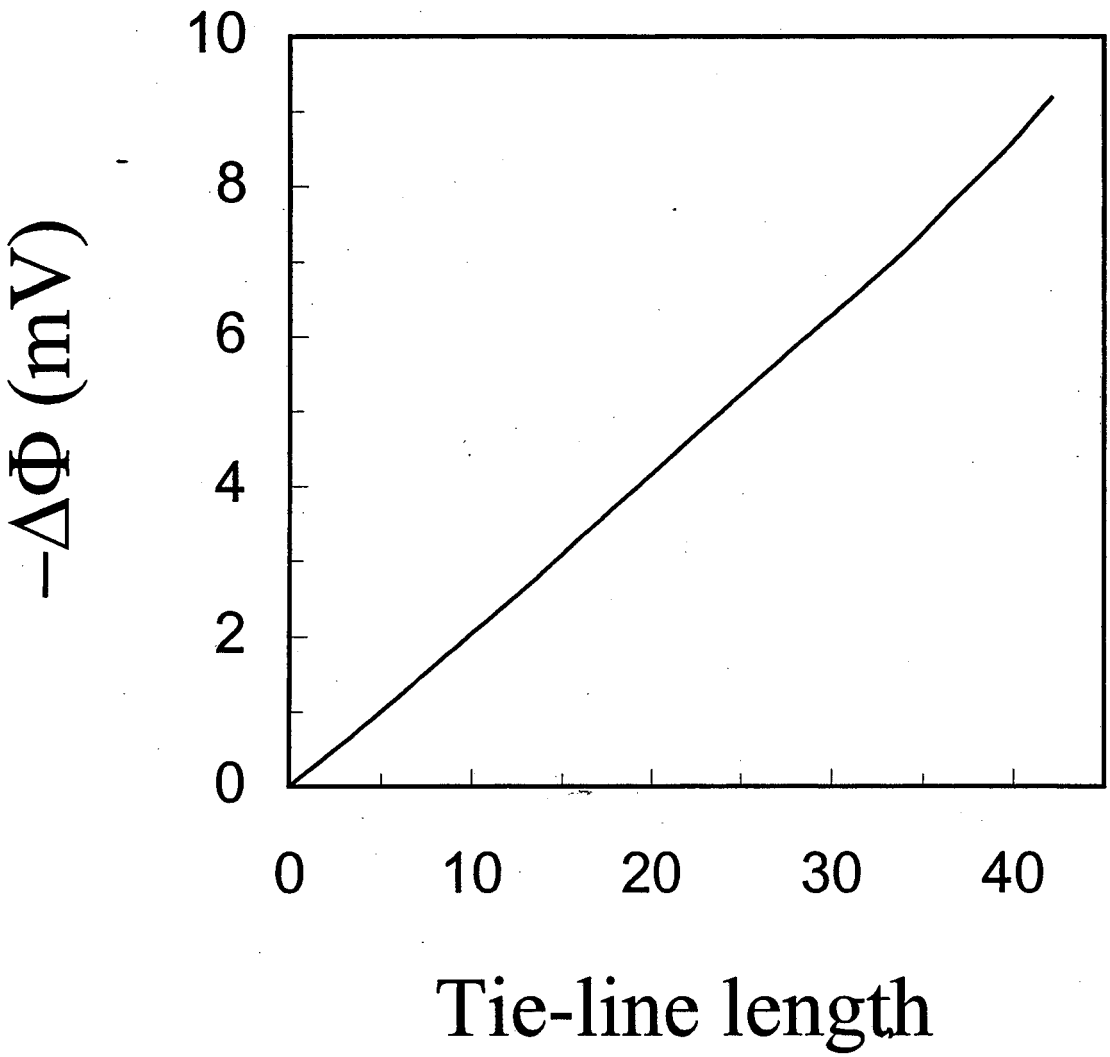

Fig.5

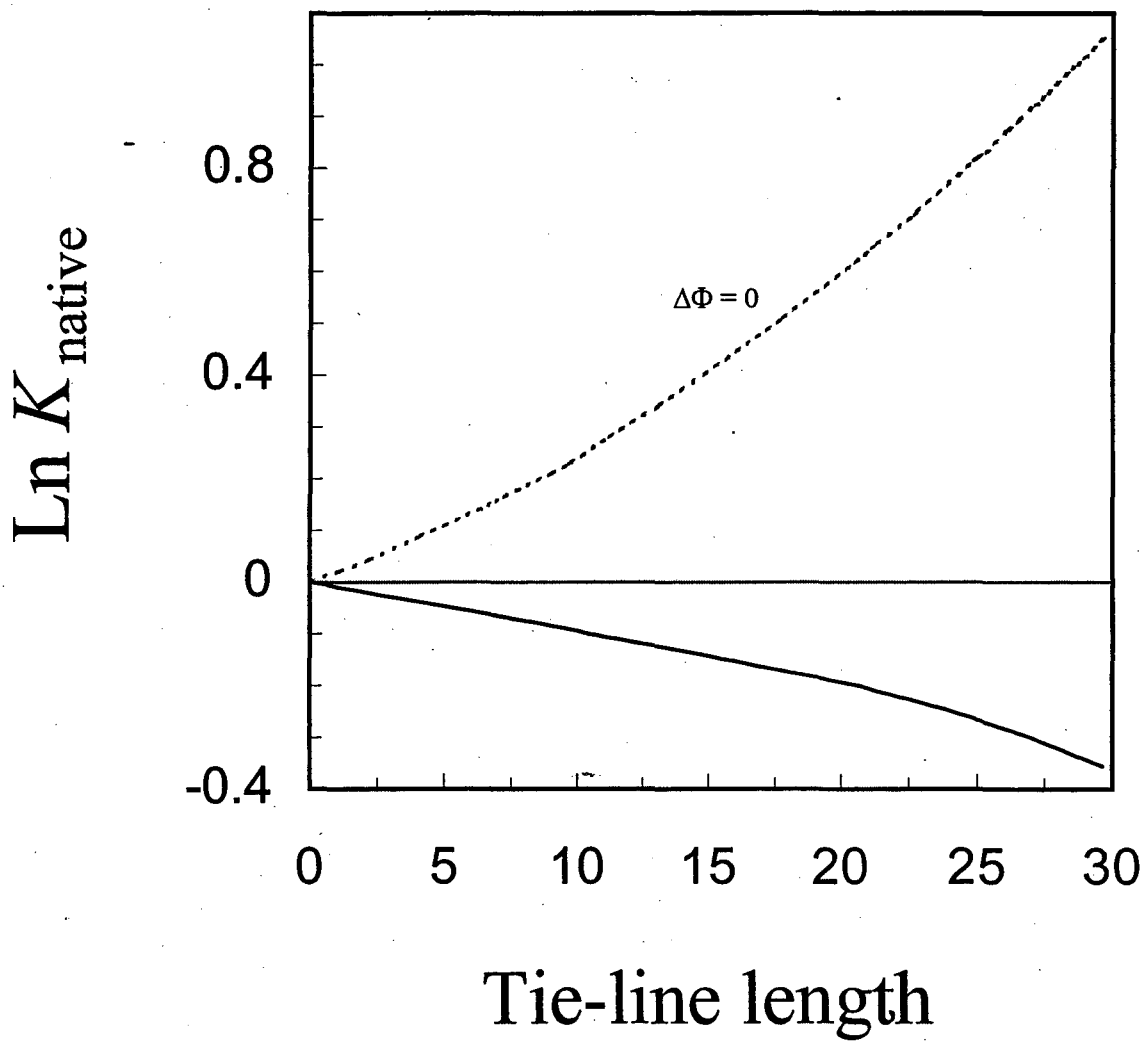
0.8
0.4
0
-0.4
Ln K_{native}
$\Delta\Phi = 0$
0
5
10
15
20
25
30
Tie-line length

Fig-

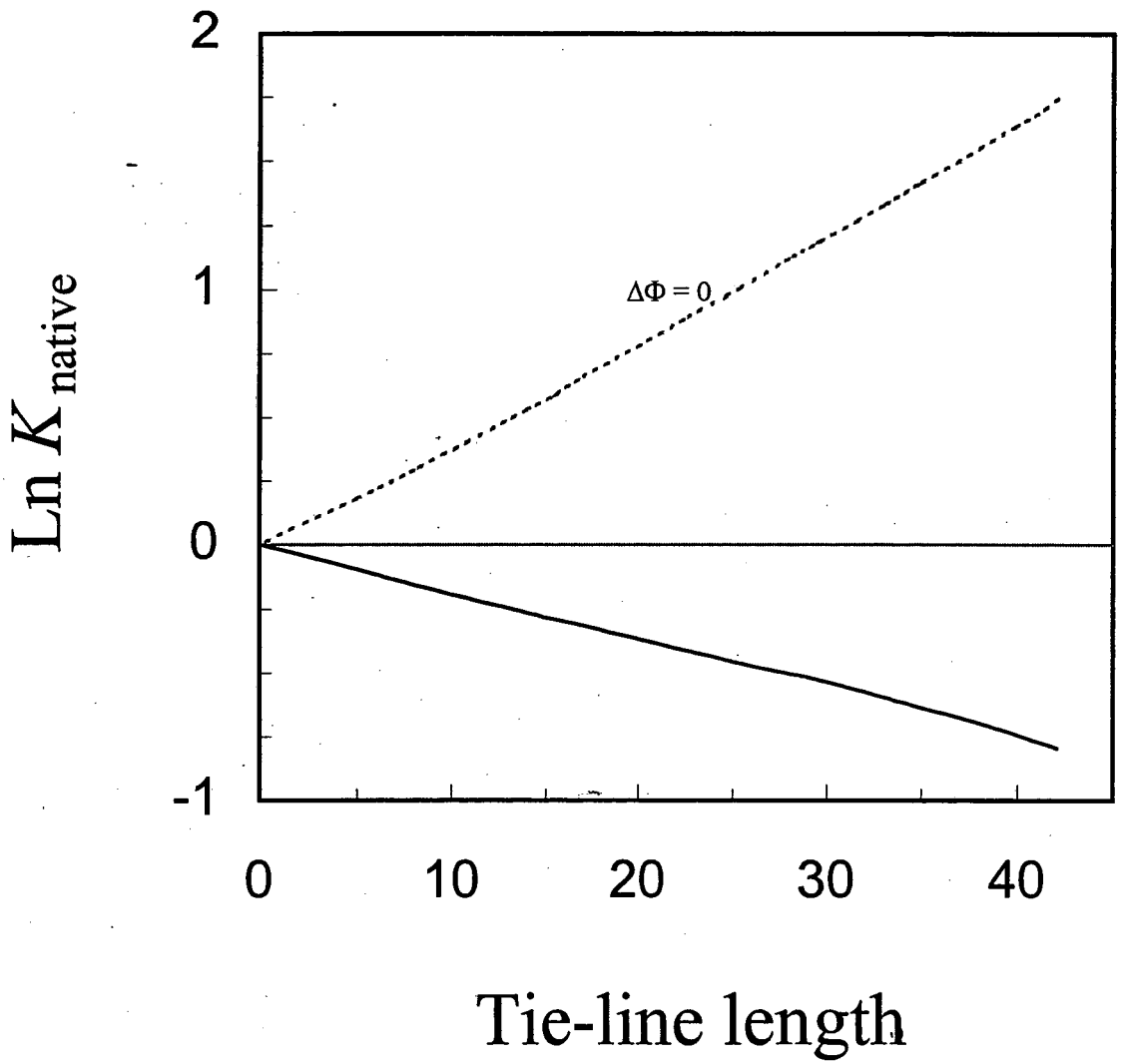

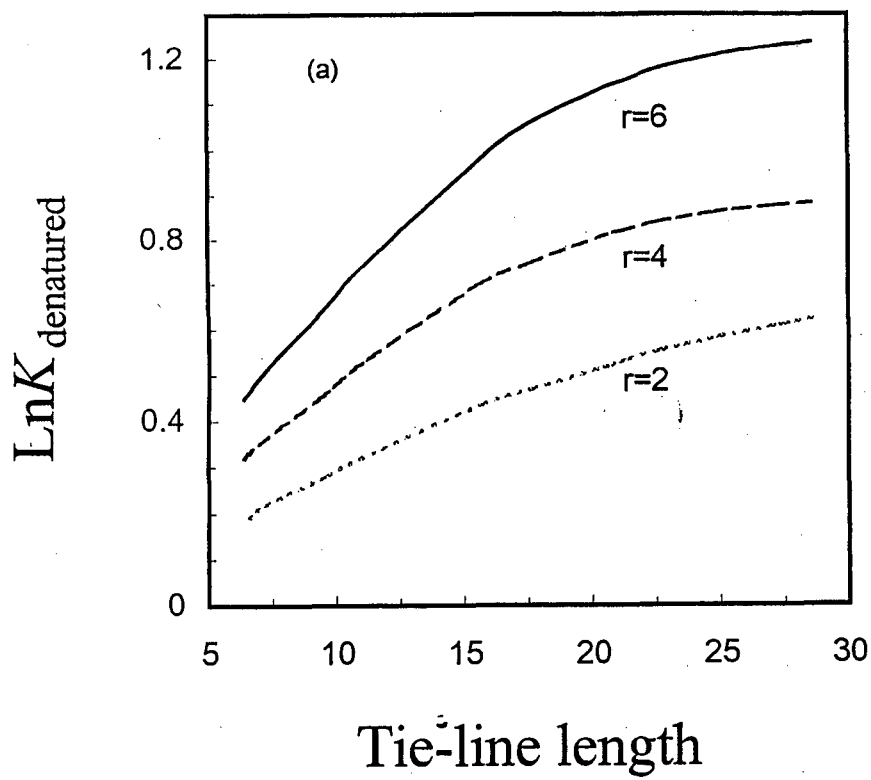
(a)
r=6
r=4
r=2
1.2
0.8
0.4
0
5
10
15
20
25
30
LnK denatured
Tie-line length

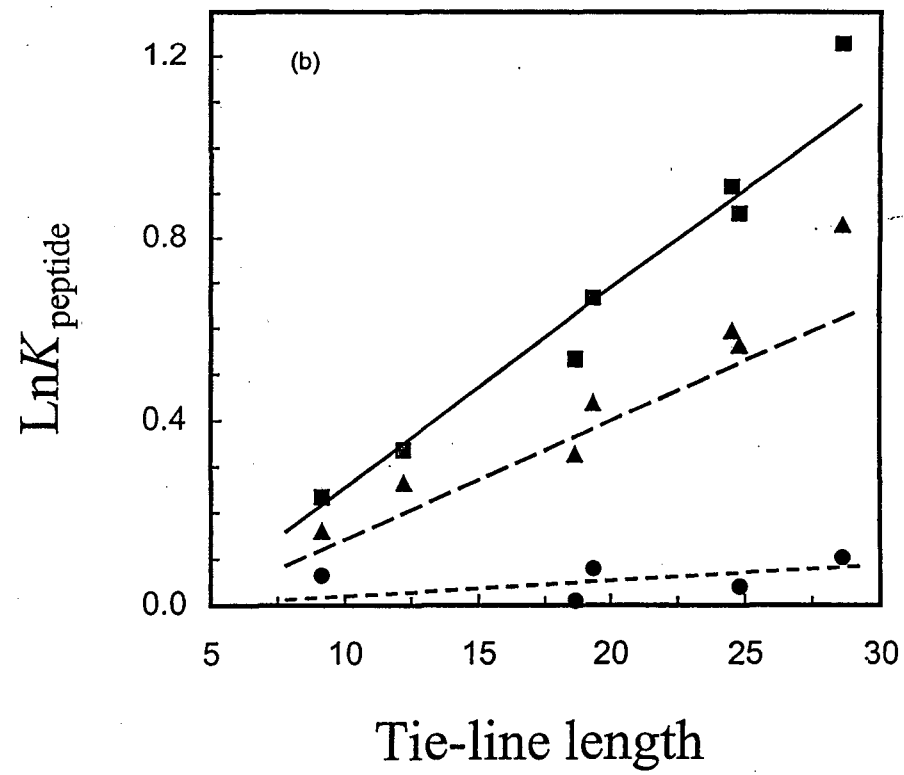
(b)
1.2
0.8
0.4
0.0
5
10
15
20
25
30
LnK peptide
Tie-line length

Fig. 7

Fig

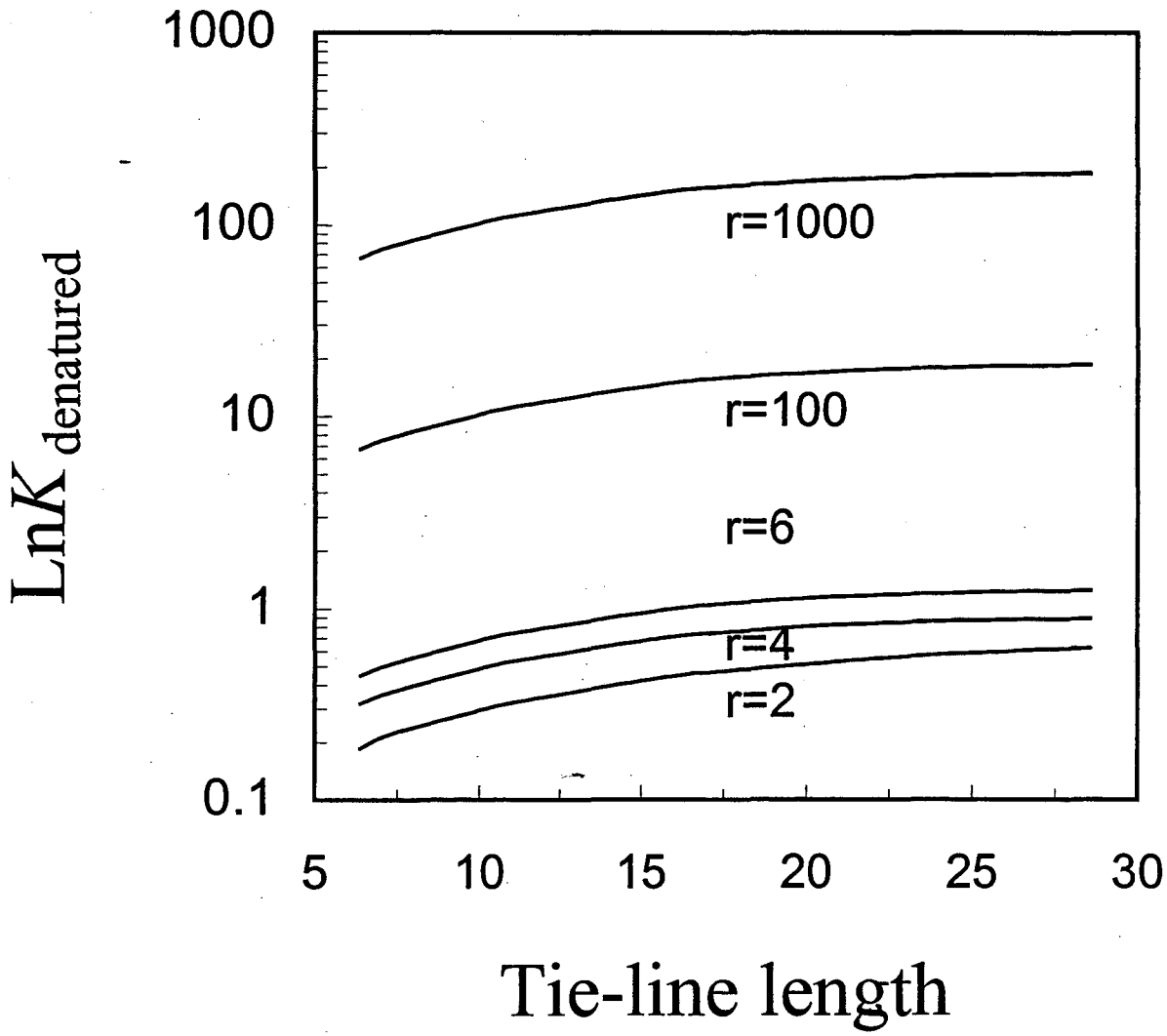
1000
100
10
1
0.1
Ln$K_{denatured}$
r=1000
r=100
r=6
r=4
r=2
5
10
15
20
25
30
Tie-line length

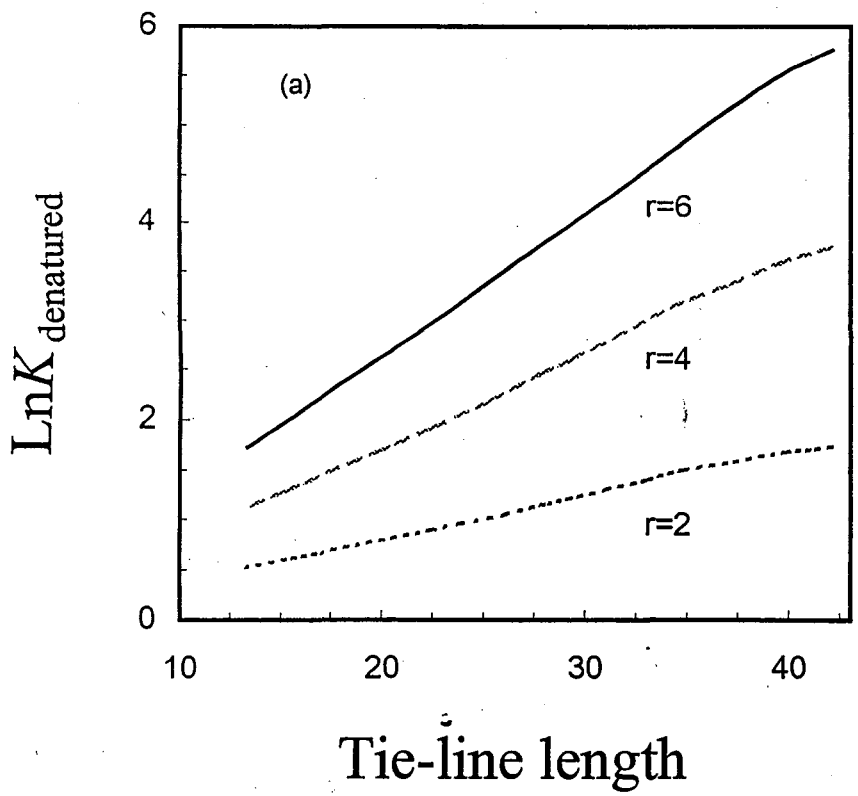
(a)
r=6
r=4
r=2
LnK denatured
Tie-line length
0
2
4
6
10
20
30
40

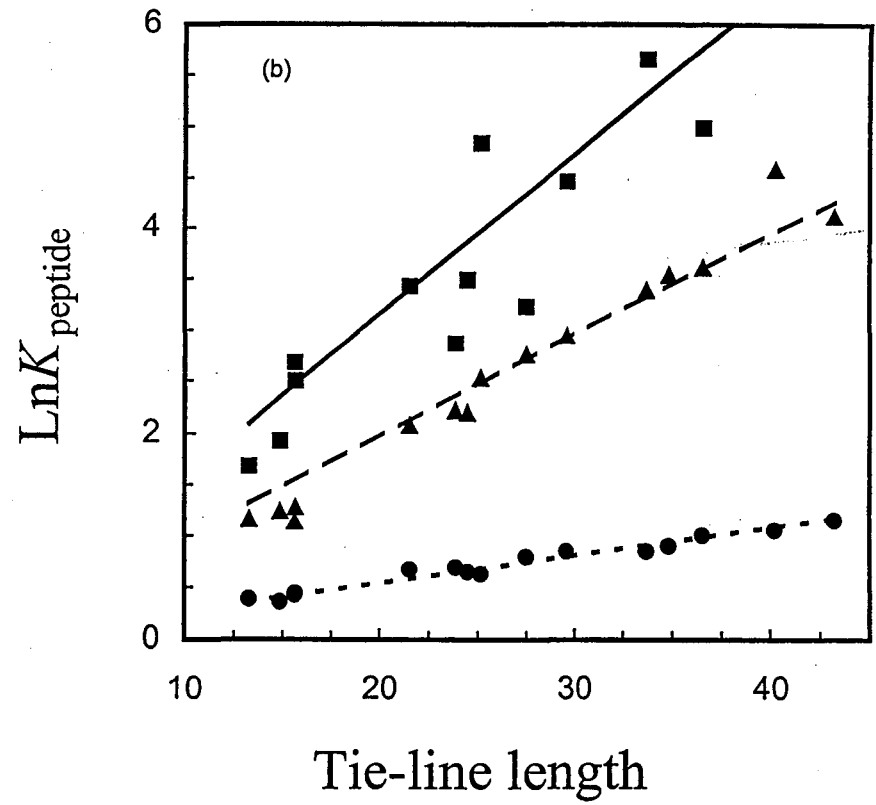
(b)
LnK peptide
Tie-line length
0
2
4
6
10
20
30
40

Fig.

Fig.1

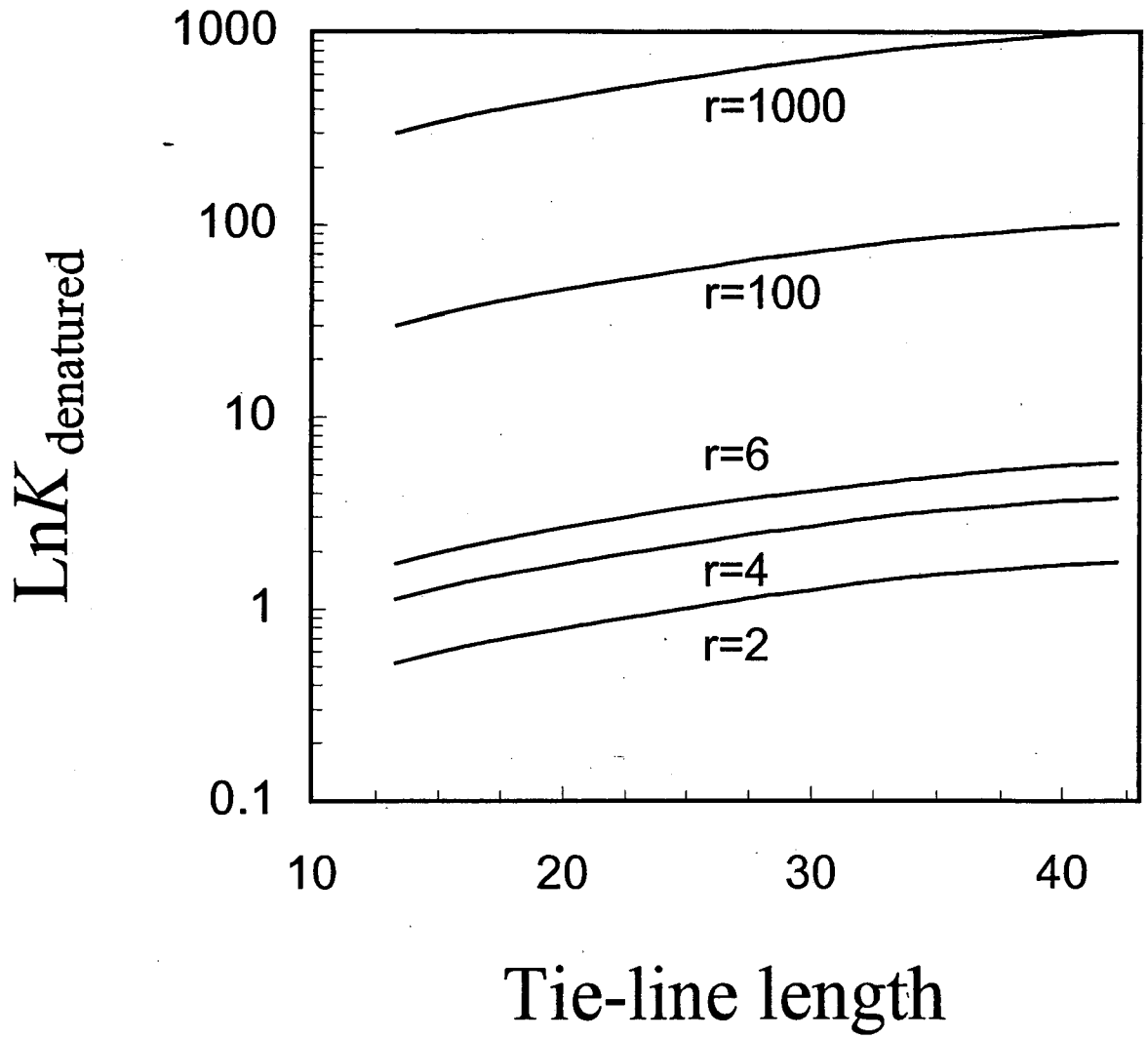
1000
100
10
1
0.1
10
20
30
40
r=1000
r=100
r=6
r=4
r=2
LnK denatured
Tie-line length

Ernest Orlando Lawrence Berkeley National Laboratory
One Cyclotron Road | Berkeley, California 94720

Prepared for the U.S. Department of Energy under Contract No. DE-AC03-76SF00098